# Sorption Isotherm, Glass Transition, and Diffusion Coefficient of Polyacrylamide/Water Solutions

David Alonso de Mezquia,[†] Frédéric Doumenc,*[‡] and M. Mounir Bou-Ali[†]

[†]Mechanical and Manufacturing Department, Engineering Faculty of Mondragon Unibertsitatea, Loramendi 4 Apdo. 23, 20500 Mondragon, Spain

[‡]UPMC Université Paris 06, Université Paris-Sud, CNRS, Laboratoire FAST, Bâtiment 502, Campus Universitaire, Orsay F-91405, France

ABSTRACT: The sorption isotherm, the glass transition, and the mutual diffusion coefficient of polyacrylamide/water solutions are obtained experimentally. All of these parameters are measured in the concentrated regime by gravimetric experiments. The mutual diffusion coefficient is also measured at high solvent concentrations by the sliding symmetric tubes technique. Three different polyacrylamide batches differing in their molar mass have been characterized. The results are expressed in terms of simple empirical correlations, suitable for use in process modelization or numerical simulations.
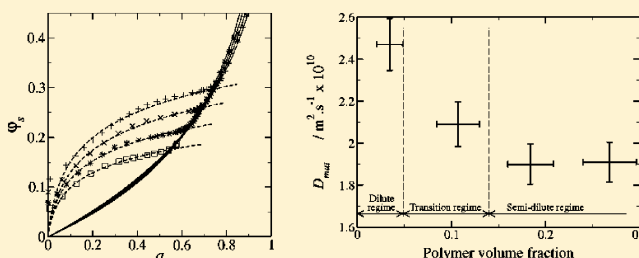
INTRODUCTION

Thermodynamic properties of polymer solutions are of great interest for both industrial processes and fundamental research. For example, the saturated vapor pressure and mutual diffusion coefficient, which strongly depend on solvent concentration, are needed for the design of industrial dryers used in the coating industry[1−3] or for membranes formation processes.[4] More fundamental issues like hydrodynamic instabilities[5] or wetting phenomena[6,7] in drying polymer solutions also require such characteristics.

The present article is dedicated to the characterization of polyacrylamide (PAAm)/water solutions. Gravimetric experiments allowing swelling and deswelling of a polymer film in a controlled solvent vapor are used for the investigation of the saturated vapor pressure as a function of concentration and temperature. The solvent activity and the polymer volume fraction at glass transition are deduced from the desorption isotherm at several temperatures. Data obtained in the rubbery regime allow the determination of the polymer−solvent interaction parameter, using the well-known Flory−Huggins model. This model is then modified to take into account the effect of viscoelastic stress on the solvent activity in the glassy regime.

Finally, the mutual diffusion coefficient is measured at room temperature, on one hand in the concentrated regime using the same experimental setup and on the other hand at high solvent concentrations using a different experimental technique called the sliding symmetric tube technique.

SYSTEM CHARACTERIZATION

Pure Polymer. Characteristics of polyacrylamide (PAAm) used in the present study are listed in Table 1. The three batches differ in their molar mass. The weight average molar mass M_w has been obtained from the manufacturer for batches

Table 1. Characteristics of PAAm (NA Stands for Not Available)

batch no.	1	2	3
supplier	Sigma-Aldrich	Polysciences, Inc.	Biovalley
catalog no.	434949	19901	02806
product form	50 wt % aqueous solution	10 wt % aqueous solution	powder
M_w/kg·mol^{-1}	22.4	600−1000	5000−6000
M_w/M_n	3.5	11	NA
T_g/K	449	451	460
φ^*_p	0.049−0.14	NA	0.0054−0.0094
$[\mu]$/m^3·kg^{-1}	0.014	NA	6.7

2 and 3. The polydispersity is defined as M_w/M_n, M_n being the number average molar mass. The polydispersity of batch 2 comes from ref 8. For batch 1, M_w and M_n have been measured by gel permeation chromatography (GPC) at Laboratory PMMD (ESPCI, France). This laboratory also measured the glass transition temperature T_g of pure polymers by differential scanning calorimetry. There are no significant differences between the three polymers, the uncertainty in T_g being ± 7 K, and these glass transition temperatures are close to the value T_g = 461 K reported in *Polymer Data Handbook*.[9]

Aqueous Solutions. The theta temperature of aqueous solutions is 235 K,[9] so they are stable in the whole range of temperature investigated in this study, (283 to 328) K. Crystallization is not expected (amorphous system)[9] and has not been detected in our experiments.

The solvent mass fraction ω_s is defined as the ratio of the solvent mass M_s over the total mass of the solution: $\omega_s = M_s/(M_s + M_p)$ with M_p as the mass of polymer. $\omega_p = (1 - \omega_s)$ is the polymer mass fraction. The solution specific volume $\bar{v}$ has been measured as a function of ω_p by an Anton Paar 5000 vibrating tube densimeter with a relative uncertainty of $5 \cdot 10^{-6}$ (temperature $T = 298$ K, polymer from batch 1). The relative uncertainty on ω_p due to sample preparation is lower than $3 \cdot 10^{-5}$. Figure 1 shows that $\bar{v}$ varies linearly with ω_p. This result
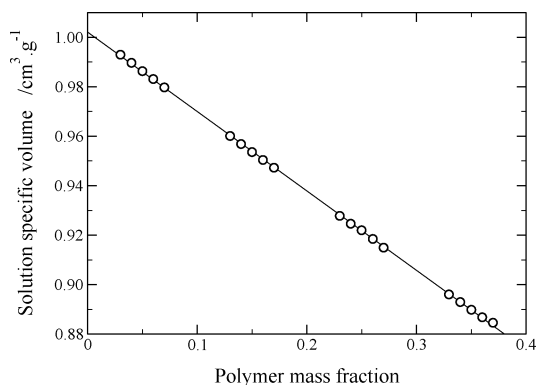
Figure 1. Solution specific volume $\bar{v}$ as a function of polymer mass fraction ω_p at $T = 298$ K (polymer from batch 1). O, experimental points; solid line, linear fit.

supports the assumption of constant partial specific volumes $\bar{v}_s$ and $\bar{v}_p$ (respectively of solvent and polymer) since $\bar{v}$ is given by

$$\bar{v} = \bar{v}_s - \omega_p(\bar{v}_s - \bar{v}_p) \tag{1}$$

A linear fit performed on data of Figure 1 gives $\bar{v}_s = 1.0021$ $cm^3 \cdot g^{-1}$ and $\bar{v}_p = 0.681$ $cm^3 \cdot g^{-1}$. The value of $\bar{v}_s$ is very close from the value 1.0030 $cm^3 \cdot g^{-1}$ reported for water,[10] and the value of $\bar{v}_p$ is consistent with the data collected from the literature,[9] ranging from 0.674 $cm^3 \cdot g^{-1}$ to 0.716 $cm^3 \cdot g^{-1}$.

The solvent volume fraction φ_s is derived from the solvent mass fraction ω_s assuming volume additivity:

$$\varphi_s = \frac{\omega_s \bar{v}_s / \bar{v}_p}{1 - \omega_s(1 - \bar{v}_s / \bar{v}_p)} \tag{2}$$

Variations of the ratio $\bar{v}_s / \bar{v}_p$ with temperature and polymer molar mass are neglected. The polymer volume fraction φ_p is given by $\varphi_p = 1 - \varphi_s$.

Using solutions of various concentrations, the polymer volume fraction at critical entanglement φ^*_p and the intrinsic viscosity $[\mu]$ have been obtained from viscosity measurements performed with a low shear 30 rheometer at room temperature (see values in Table 1). Due to high polydispersity of polymers used in this study, we are not able to provide a single value of φ^*_p, but a concentration range corresponding to the transition between the dilute and the semidilute regimes. It is well-known that the intrinsic viscosity dependence on the polymer molar mass can be described by a power law. In the case of batch 1, using the value of $[\mu]$ in Table 1 and the sets of coefficients reported by Scholtan,[11] Klein and Conrad,[12] or Munk et al.,[13] we obtain molar mass estimations of (15, 21, or 9.2) $kg \cdot mol^{-1}$, respectively, which are rather close from the value $M_w = 22.4$ $kg \cdot mol^{-1}$ measured by GPC. On the contrary, the same method applied to batch 3 leads to molar mass estimations 10 times higher than the value provided by the manufacturer. Anyway,

this batch is only used in experiments which are expected to be weakly sensitive to the molar mass (sorption isotherm or diffusion coefficient in the concentrated regime). This weak dependency is systematically checked by comparison with results from batch 2.

■ EXPERIMENTAL SETUP

Gravimetric Experiments. *Setup Characteristics.* The sorption isotherm and the diffusion coefficient in the concentrated regime are obtained using an experimental setup which consists of an accurate balance coupled with a vapor chamber whose temperature and pressure are controlled. The sample is hung in the chamber, and changing the solvent vapor pressure allows for swelling or drying of the polymer film. The gravimetric setup is a Hiden IGA system based on a precise balance. The chamber is a stainless steel cylinder with a diameter of 34.5 mm and a height of 300 mm. The temperature is regulated with a fluid circulating in the outer wall of the chamber from a thermostatted bath. The temperature is measured by a platinum resistance thermometer (Pt 100) located near the sample. The uncertainty in the temperature measurement is $\pm$ 0.1 K, and the temperature stability is better than $\pm$ 0.05 K. The chamber is connected through various valves to a vacuum pump on one hand and to a solvent tank on the other hand, where liquid solvent is in equilibrium with its vapor at 328 K. The pressure is regulated with a PID controller, and the pressure stability is better than 2 Pa. The solvent vapor is the only gas present in the chamber, so the total pressure and the solvent vapor pressure are the same. The pressure is measured with a manometer (relative error 0.3 %). The mass measurement noise is about 1 μg, and the reproducibility (same measurement performed at various times) is about 10 μg.

Determination of Solvent Activity. The saturated vapor pressure of pure water has been estimated from Antoine's law:

$$P_{vs0} = \exp\left(A - \frac{B}{T - C}\right) \tag{3}$$

with P_{vs0} in Pa, T the absolute temperature in K, $A = 23.5334$, $B = 4023.44$, and $C = 38.076$ (coefficients obtained from the Hiden microbalance software). We tested this relation by comparison with data reported by Riddick et al.[14] and found a relative error lower than 0.4 % in the temperature range from (273 to 373) K. Assuming that water vapor behaves like an ideal gas, the water activity is given by the classical relation $a = (P_{vs}/P_{vs0})$, with P_{vs} the vapor pressure measured above the solution. The relative error in the activity due to the uncertainty in P_{vs} and P_{vs0} is lower than 1.4 %.

Sample Preparation. For gravimetric experiments, aqueous solutions were prepared using ultrapure water (resistivity 18.2 MΩ.cm). Then polymer films of uniform thickness were obtained by slow drying of the aqueous solution in glass dishes. The drying time (typically a few days) was controlled by putting the dish in a box, with a small aperture to allow slow vapor diffusion outside the box. The initial concentration was chosen to get a solution initial viscosity in the range from (0.1 to 1) Pa·s. Indeed, a too-large viscosity induces formation of air bubbles, while hydrodynamic instabilities leading to wrinkle formation[5] are promoted by a too-small viscosity (for the highest molar mass, good results were obtained with an initial polymer mass fraction approximately equal to 0.01). The initial thickness (typically from 1 mm to a few centimeters) is adjusted to get the desired dried sample thickness. After drying,

the film is taken off from the dish, and a disk of diameter $D =$ 20.0 $\pm$ 0.1 mm is cut with a hollow punch. This operation is performed in an atmosphere of 80 % humidity to prevent formation of cracks. Then the sample is hung horizontally in the balance chamber, its two sides being exposed to solvent vapor. After the end of experiments, complete drying of the sample is achieved by placing it in an oven under vacuum during at least 10 h at 423 K. Then the film is weighed on a Sartorius balance to get the polymer mass M_p (absolute uncertainty: $\pm$ 0.1 mg). Finally, the sample dry thickness h_{dry} is estimated by the relation $h_{dry} = \bar{v}_p M_p/(\pi D^2/4)$.

The polymer mass M_p, the dry thickness h_{dry}, and the higher bound of the absolute error in ω_s (estimated from the errors in M_p and M_s) of the three samples used in gravimetric experiments are given in Table 2. The relative uncertainty on h_{dry} is estimated at $\pm$ 7 %.

Table 2. Characteristics of Samples Used in Gravimetric Experiments (See Table 1 for Batch Characteristics)

sample	1	2	3
batch	2	3	3
M_p/mg	9.5	16.8	217.5
h_{dry}/μm	21	36	470
$\Delta\omega_s$	$\leq 5 \cdot 10^{-3}$	$\leq 2 \cdot 10^{-3}$	$\leq 1 \cdot 10^{-4}$

Sliding Symmetric Tubes Technique. *Setup Characteristics.* The determination of the mutual diffusion coefficient D_{mut} at high solvent concentrations has been carried out by the sliding symmetric tubes (SST) technique, which has been developed recently at Mondragon Unibertsitatea for the determination of mutual diffusion coefficient of binary systems in the liquid phase. This technique has been validated by measuring the mutual diffusion coefficient of several well-documented systems.[15] The difference with data from literature was less than 3 %.

The SST technique consists of two identical vertical tubes (length: 60 $\pm$ 0.01 mm, diameter: 9 $\pm$ 0.01 mm), each containing a solution with slightly different concentrations (the concentration difference between the tubes has to be small enough to make the variation of diffusion coefficient negligible). The solution with higher density is placed in the lower tube to eliminate convection. The temperature of the tubes is controlled by introducing them in a water bath, regulated by a Lauda RCS thermostatic bath. All of the walls of the bath are thermally insulated so that the temperature variations inside the bath are lower than 0.1 K. A couple of tubes can be set in two positions: the "faced" configuration allows mass transfer between tubes, while the "separated" configuration interrupts it (in the latter case, each tube is closed impermeably).

Measurement of Average Concentration as a Function of Time. In these experiments, we used batch 1 polymer, purchased as an aqueous solution of 0.50 polymer mass fraction. The desired concentration is obtained by adding the appropriate amount of bidistilled water, using a 10 mg precision microbalance. At the beginning of the experiment, 10 couples of tubes are placed in the water bath in a "separated" configuration. We first wait a time long enough to be sure that thermal equilibrium is reached (typically 48 h), and then the tubes are switched to the "faced" configuration by an external screw, allowing the diffusion to begin. The couples of tubes are then switched back to the "separated" configuration,

one after the other, at different times (see Figure 2). After homogenization of the concentration field by shaking, the
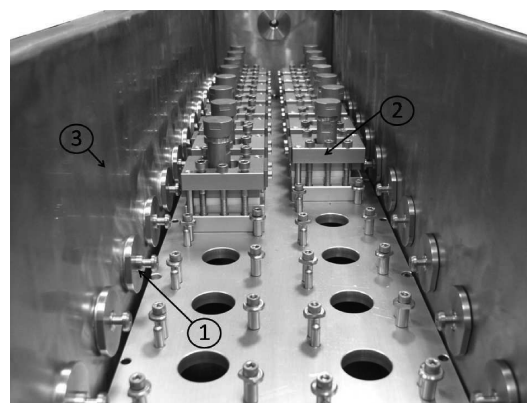
Figure 2. Photograph of the chamber containing the sets of tubes. (1) Screws used to switch between "faced" and "separated" positions, (2) sets of sliding tubes, (3) insulated walls.

density of the solution is measured by the Anton Paar 5000 densimeter, which allows us to know the average solution density in each tube (maximum solution viscosity allowed with this densimeter: 70 mPa·s). Finally, the average concentration inside each tube is determined from density measurements (see data in Figure 1). This gives the average polymer concentration in each tube at the time corresponding to the interruption of mass transfer between the tubes.
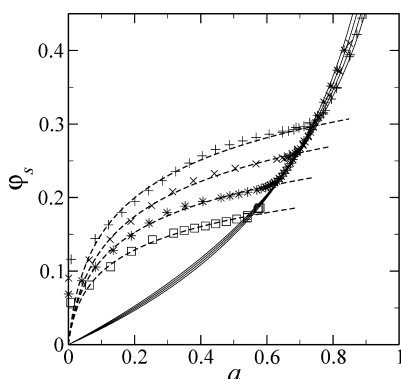
■ SORPTION ISOTHERM

As already mentioned, sorption isotherms are obtained from gravimetric experiments. The experimental protocol must take into account that dry PAAm is glassy at temperatures investigated in this study. To erase history effects,[16,17] we always start the experiments at a vapor pressure high enough to bring the sample above the glass transition, in a state of thermodynamic equilibrium (rubbery regime). Then we perform a series of decreasing differential steps of solvent vapor pressure. When the sample is still in the rubbery regime, the asymptotic value reached at the end of the step gives the equilibrium solvent concentration in the film, corresponding to the imposed solvent vapor pressure. Below the glass transition (i.e., in the glassy regime), a steady state can no longer be reached in a reasonable time. In that case, the duration of each step is fixed at three hours, and the desorption isotherm is built using the mass at the end of each step.

The experimental desorption isotherms obtained for the different temperatures are represented in Figure 3. The glass transition corresponds to the sudden change of slope in the function $\varphi_s(a)$. The glassy regime is characterized by an excess of solvent, compared to thermodynamic equilibrium. The extension of the glassy regime is reduced when the temperature is increased.

The rubbery domain can be described by the classical Flory–Huggins law:[18]

$$a = (1 - \varphi_p)\exp(\varphi_p + \chi\varphi_p^2) \tag{4}$$

where χ is the Flory–Huggins interaction parameter which characterizes the affinity between the solvent and the polymer. To determine χ as a function of φ_s and T, we first make a rough determination of φ_{sg} and a_g (with φ_{sg} and a_g the solvent volume

Figure 3. Desorption isotherm: solvent volume fraction φ_s as a function of activity a (sample 2). +, 283 K; ×, 298 K; ∗, 313 K; □, 328 K; solid lines, fit of the equilibrium regime (eq 4); dashed lines, fit of the glassy regime (eq 6).

fraction and the activity at glass transition, respectively), based on the change of slope in the function $\varphi_s(a)$. Then χ is fitted using the data such that $\varphi_s > \varphi_{sg}$. Assuming that χ varies linearly with φ_s and T gives a good description of experimental data. We obtain:

$$\chi(\varphi_s, T) = 0.482 - 0.150\varphi_s + 3.3 \cdot 10^{-3}(T - 298)$$
$$- 1.44 \cdot 10^{-2}\varphi_s(T - 298) \quad (5)$$

This empirical law is valid in the rubbery regime and in the parameter range covered in the experiments, that is, $a_g \leq a \leq 0.9$ and 283 K $\leq T \leq$ 328 K. In this validity domain, the Flory−Huggins interaction parameter varies from 0.32 to 0.48. Polymer of batch 3 was used in the experiments, but we do not expect any significant effect of molar mass on χ in that concentration range. Indeed, we checked that eqs 4 and 5 predict in a very satisfactory way, at $T = 298$ K, the rubbery regime of a solution made from batch 2 polymer.

We can account for the excess of solvent in the glassy regime by using the simple model developed by Leibler and Sekimoto.[19] This model relates the excess of solvent to elastic properties in glassy regime. The elastic energy associated with the sample deformation under volume variation is taken into account via an osmotic bulk modulus K_g, which is assumed to be constant. This leads to a modified Flory−Huggins equation, valid below the glass transition:

$$a = (1 - \varphi_p)\exp\left[\varphi_p + \chi\varphi_p^2 - \frac{\bar{v}^{\circ}_s K_g}{RT}\log\left(\frac{\varphi_p}{\varphi_{pg}}\right)\right] \quad (6)$$

with $\bar{v}^{\circ}_s$ as the solvent molar volume, R as the ideal gas constant, and φ_{pg} as the polymer volume fraction at glass transition.

Parameters K_g and φ_{pg} are fitted using eq 6 and the experimental data in the glassy regime. Then the activity at glass transition a_g is obtained by setting $\varphi_p = \varphi_{pg}$ in eq 6 (this leads to a slightly more accurate estimation of φ_{pg} and a_g than the values previously obtained by slope inspection). We can see in Figure 3 that the fit is quite good, except at very low solvent volume fractions. It is worthwhile to note that a constant value of K_g gives a good agreement with the experimental data over a wide range of solvent volume fraction φ_s, so a direct dependence of K_g on φ_s cannot be established in a straightforward way. As already pointed out by Saby-Dubreuil et al.,[20] the value of K_g

obtained from this method is an average value which corresponds to the concentration range of the fit and depends strongly on the polymer matrix state.

The results are presented in Table 3. By comparing samples 1 and 2 at $T = 298$ K, we see that the effect of the molar mass

Table 3. Activity a_g and Solvent Volume Fraction φ_{sg} at Glass Transition, with Osmotic Bulk Modulus K_g in a Glassy Regime, as a Function of Temperature (The Relative Uncertainty in K_g Is of the Order of 10 %)

temperature/K	283	298	298	313	328
sample	2	2	1	2	2
φ_{sg}	0.30	0.26	0.28	0.22	0.18
a_g	0.75	0.69	0.72	0.62	0.54
K_g/GPa	1.08	1.25	1.04	1.65	2.22

on φ_{sg}, a_g, and K_g is very weak, at the limit of the uncertainty ranges. On the other hand, increasing the temperature from (283 to 328) K induces a significant effect on these parameters. We observe that the higher the temperature, the lower φ_{sg} and a_g, as expected. At the contrary, K_g increases significantly with the temperature (it is multiplied by 2 when the temperature goes up by 45 K). This means that the system stiffness in the glassy regime increases with temperature. This nontrivial behavior can be related to observations made by Saby-Dubreuil et al.[20] on the desorption isotherm of PMMA-PnBMA statistical copolymers in toluene (similar protocol than the present study). These authors found that, at a fixed temperature, increasing the amount of the monomer with the lowest glass transition temperature (nBMA) leads to a decrease of φ_{sg} and a_g, but to an increase of K_g, while the opposite behavior was noticed on annealed samples (decrease of K_g when increasing the nBMA amount). This observation confirms that K_g is not an intrinsic property of the system but also depends on its history.

■ DIFFUSION COEFFICIENT

Concentrated Regime. The time evolution of the mass of the film in response to an imposed step of the solvent vapor pressure gives access to the mutual diffusion coefficient, through a suitable model of the swelling kinetics. This method of measurement of mutual diffusion coefficients of polymer solutions has been widely used in the literature, for rubbery systems[21,22] as well as glassy systems.[23−27] This method can only be used if at least a part of the sorption kinetics is driven by polymer/solvent mutual diffusion. This is not the case at high vapor pressure, since it has been shown that in this regime the kinetics are dominated by thermal effects.[28] This is why the measurement of polymer/solvent diffusivity by gravimetry is usually restricted to the concentrated regime. Moreover, in the case of glassy systems, the model must take into account viscoelastic relaxation, coupled with diffusion. Like for sorption isotherms, we always perform decreasing vapor pressure steps, starting from thermodynamic equilibrium. However, the step duration is not fixed but adapted to be much longer than the diffusion time. This condition is necessary to distinguish the mass evolution due to diffusion from the effect of viscoelastic stress relaxation.[29] For the thickest samples at low vapor pressure, the step duration can go to several days.

The sample being glassy in the concentration range covered by the experiments, the variation of mass after the pressure step is due to the coupling between solvent diffusion and polymer

matrix relaxation. Indeed, in the glassy regime, viscoelastic relaxation involves characteristic times of the same order of the experiment duration and must be incorporated into the modeling of kinetics. We therefore used the classical model by Long and Richman,[30] which takes into account the relaxation of polymer matrix through its effect on solvent solubility at the film–vapor interface. After the pressure step, the solvent concentration at the interface is assumed to vary in the following way:

$$\Delta c_{int}(t) = \Delta c_d + (\Delta c_\infty - \Delta c_d)[1 - \exp(-t/\tau_r)] \quad (7)$$

where $\Delta c_{int}(t)$ is the variation of solvent concentration at the interface as a function of time t, Δc_d is the "quasi-equilibrium" concentration variation (the asymptotic concentration variation if the only mechanism is diffusion), Δc_∞ the equilibrium concentration variation, and τ_r the relaxation characteristic time. The solvent transport inside the film is described by the Fick equation. If the pressure step is small enough, the solvent contents varies very little, so the mutual diffusion coefficient D_{mut} and the sample thickness h can be considered as constant. The diffusion equation thus reads:

$$\frac{\partial \Delta c}{\partial t} = D_{mut} \frac{\partial^2 \Delta c}{\partial x^2} \quad \text{for} \quad 0 < x < h/2 \quad (8)$$

where Δc is the local solvent concentration variation since the pressure step and x the distance from the symmetry plane in the center of the sample. The second boundary condition results from symmetry:

$$\frac{\partial \Delta c}{\partial x} = 0 \quad \text{for} \quad x = 0 \quad (9)$$

and the initial condition is $\Delta c = 0$. Finally, the variation of solvent mass can be obtained by integration over the sample thickness:

$$\Delta m_s(t) = \int_0^{h/2} c(x, t)dx \quad (10)$$

Equations 7 to 10 can be solved analytically by use of the Laplace transform.[29] The parameters D_{mut}, τ_r, Δc_d, and Δc_∞ are then estimated by least-squares optimization (Levenberg–Marquardt algorithm), to minimize the differences between the theoretical and the experimental mass variations.

The Long and Richman model is well-known to reproduce in a very satisfactory way the shape of the different types of kinetics encountered in the glassy regime,[26,30] with the advantage of simplicity and low computational time. Its drawback is the naive representation of viscoelastic relaxation, based on a unique characteristic time. Indeed, the relaxation of the polymer matrix in the glassy regime involves a broad distribution of characteristic times, running on several decades.[31] In a previous study,[26] we showed that changing the exponential in eq 7 into a stretched exponential to introduce a time distribution into the relaxation model leads to different values of Δc_∞ and τ_r but does not alter significantly the estimated values of Δc_d and D_{mut}. Although oversimplified, this modeling of relaxation succeeds in separating the effect of diffusion from the effect of relaxation and therefore is consistent with our aim which is the determination of D_{mut}.

The parameter τ_r having no physical sense, we do not present it in the following (in fact, it reflects the part of the time distribution which is observable during the experiments, so its value is always of order of the experimental time τ_{exp}; see ref 27 for details).

The typical kinetics is presented in Figure 4. The absolute value of mass variation is plotted as a function of square root of
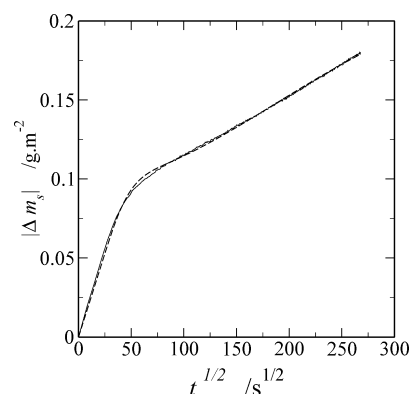
Figure 4. Drying kinetics at 298 K. Sample 2, $h_{dry} = 36$ mm, $\varphi_{si} = 0.142$, $\varphi_{sf} = 0.135$, $D_{mut} = 1.6 \cdot 10^{-13}$ m^2·s^{-1}, $\tau_r = 6.9 \cdot 10^4$ s, $\tau_{exp} = 7.2 \cdot 10^4$ s. Solid line, experimental data; dashed line, numerical simulation (fit).

time. The change of slope around $(t)^{1/2} \approx 50$ s$^{1/2}$ delimits two regimes: the first one is dominated by diffusion, the second one by viscoelastic relaxation. The very good fit observed in that figure is representative of all of the experiments.

The same procedure has been repeated for various initial and final vapor pressures and different sample thicknesses. The values obtained for D_{mut} are presented in Table 4, as

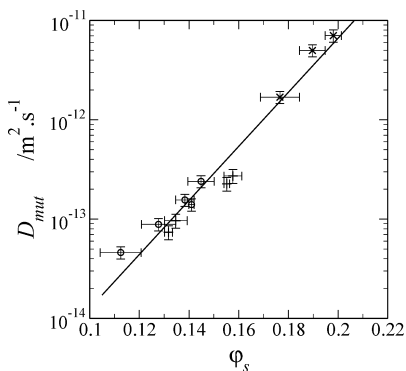**Table 4. Mutual Diffusion Coefficient D_{mut} in the Concentrated Regime (Relative Uncertainty: ± 15 %)**

			D_{mut} m^2·s^{-1}
Sample 1, $h_{dry} = 21$ μm			
$\overline{\varphi}_s$	φ_{si}	φ_{sf}	
0.1347	0.1393	0.1301	9.6·10^{-14}
0.1318	0.1301	0.1334	7.4·10^{-14}
0.1552	0.1541	0.1563	2.3·10^{-13}
0.1577	0.1613	0.1541	2.7·10^{-13}
Sample 2, $h_{dry} = 36$ μm			
$\overline{\varphi}_s$	φ_{si}	φ_{sf}	D_{mut} m^2·s^{-1}
0.1125	0.1207	0.1043	4.6·10^{-14}
0.1278	0.1346	0.1209	8.9·10^{-14}
0.1411	0.1400	0.1421	1.4·10^{-13}
0.1384	0.1421	0.1346	1.6·10^{-13}
0.1449	0.1501	0.1396	2.4·10^{-13}
Sample 3, $h_{dry} = 470$ μm			
$\overline{\varphi}_s$	φ_{si}	φ_{sf}	D_{mut} m^2·s^{-1}
0.1766	0.1845	0.1687	1.7·10^{-12}
0.1897	0.1949	0.1845	5.0·10^{-12}
0.1981	0.2013	0.1949	7.0·10^{-12}

a function of φ_{si} and φ_{sf}, the initial and final polymer volume fraction averaged on the sample thickness, respectively.

These data have been fitted to get the following empirical relation:

$$\log_{10}(D_{\text{mut}}) = 27.23\varphi_s - 16.624 \qquad \text{for}$$

$$0.11 \le \varphi_s \le 0.20 \qquad (11)$$

The experimental values of D_{mut} are plotted in Figure 5 as a function of solvent volume fraction φ_s. D_{mut} increases by more

Figure 5. Mutual diffusion coefficient in the concentrated regime as a function of solvent volume fraction, at $T = 298$ K. Symbols, experimental values (horizontal error bars represent φ_{si} and φ_{sf}; vertical error bars represent the uncertainty on D_{mut}); solid line, linear fit (eq 11).

than two orders of magnitude when φ_s goes up by approximately 0.1. This strong sensitivity of D_{mut} on φ_s is characteristic of polymer solutions in the concentrated regime.

Semidilute and Dilute Regimes. The mutual diffusion coefficient at high concentration of solvent has been measured by the SST technique at $T = 298$ K, for polymers of batch 1. Figure 6 shows the time evolution of the average polymer
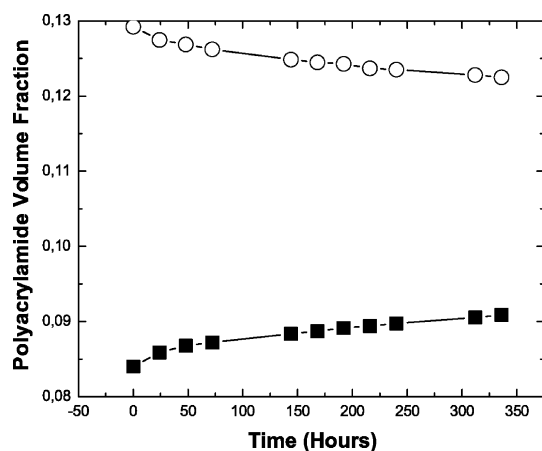
Figure 6. Time evolution of polymer volume fraction in both tubes for $\overline{\varphi}_p = 0.1072$. ■, top tube; ○, bottom tube; solid lines represent fits by eqs 12 and 13 ($T = 298$ K, polymer from batch 1).

volume fraction in each tube (upper and bottom). The polymer volume fraction averaged over both tubes $\overline{\varphi}_p$ is a constant and is equal to 0.1072 during the entire experiment.

We assume that mass transfer inside the tubes is purely diffusive (convection has been canceled by placing the heavier fluid in the bottom tube) and obey the classical Fick's law (solvent concentration being far above the glass transition, the effect of viscoelastic stress on mass transfer can be neglected).

In addition, we consider that, before contact at time $t = 0$, the concentration is uniform in each tube. Solving the diffusion equation with these assumptions leads to the expression of the average concentration in each tube as a function of time:

$$\overline{c^{\text{up}}}(t) - \frac{c_i^{\text{up}} + c_i^{\text{bot}}}{2} = \frac{8}{\pi^2}\left(c_i^{\text{up}} - \frac{c_i^{\text{up}} + c_i^{\text{bot}}}{2}\right)$$
$$\cdot \sum_{n=0}^{\infty} \frac{\exp\left(-(n + 1/2)^2 \frac{\pi^2}{L^2} D_{\text{mut}} t\right)}{(2n + 1)^2} \qquad (12)$$

$$\overline{c^{\text{bot}}}(t) - \frac{c_i^{\text{up}} + c_i^{\text{bot}}}{2} = -\frac{8}{\pi^2}\left(c_i^{\text{up}} - \frac{c_i^{\text{up}} + c_i^{\text{bot}}}{2}\right)$$
$$\cdot \sum_{n=0}^{\infty} \frac{\exp\left(-(n + 1/2)^2 \frac{\pi^2}{L^2} D_{\text{mut}} t\right)}{(2n + 1)^2} \qquad (13)$$

where $\overline{c^{\text{up/bot}}}$ (t) are the mean polymer concentrations in the upper and lower tube, $c_i^{\text{up/bot}}$ are the initial polymer concentrations in upper and lower tube, respectively, L is the length of the tube, t is the time of the experiment, and D_{mut} is the mutual diffusion coefficient. The mutual diffusion coefficient is obtained by least-squares method (Matlab routine), to minimize the difference between the model and the experimental results (see the fit in Figure 6). Typically up to 11 points are used in each experiment. This allows us to take into account experimental points from the very beginning of the experiment, which is not possible in other similar techniques like the open-ended capillary technique.[32] Another advantage of the SST is that the two tubes give independent results, which can be compared each other. Indeed, in the ideal case where the difference of initial concentrations goes to zero, the two tubes should give the same result. In all cases presented in this article, the difference between the values obtained for D_{mut} in each tube was lower than 5 %. In the following, we present the average value.

Four different polymer volume fractions have been investigated. The first one ($\overline{\varphi}_p = 0.0346$) is in the dilute regime; the second ($\overline{\varphi}_p = 0.1072$) is in the transition regime, and the two last ones ($\overline{\varphi}_p = 0.1848$ and 0.2526) are in the semidilute regime. Results are presented in Table 5 and Figure 7. The order of magnitude of D_{mut} is the same in all cases and corresponds to what is expected for polymer solutions at room temperature in that concentration range. There is no variation of D_{mut} in the semidilute regime, and then it increases by 30 % when the polymer concentration is lowered.

The mutual diffusion coefficient of PAAm/water solutions has been widely investigated in the literature, but at very low polymer volume fractions. Experimental techniques include ultracentrifuge[11] or light scattering.[33,34] The diffusion coefficient D_0 in the limit of vanishing polymer volume fraction depends on the polymer molar mass through a power law,

Table 5. Mutual Diffusion Coefficient as a Function of Polymer Volume Fraction in the Dilute and Semidilute Regimes[a]

$\bar{\varphi}_p$	φ_p^{up}	φ_p^{bot}	μ mPa·s	D_{mut} m²·s⁻¹
0.0346	0.0206	0.0486	1.6	$2.47 \cdot 10^{-10}$
0.1072	0.0844	0.1300	5.2	$2.09 \cdot 10^{-10}$
0.1848	0.1606	0.2091	17	$1.90 \cdot 10^{-10}$
0.2526	0.2400	0.2962	68	$1.91 \cdot 10^{-10}$

[a]φ_p^{up} and φ_p^{bot} are the initial polymer volume fractions in the upper and bottom tubes, respectively. $\bar{\varphi}_p$ is the polymer volume fraction averaged over both tubes. The dynamic viscosity μ at volume fraction $\bar{\varphi}_p$ is also provided for information (T = 298 K, polymer from batch 1).
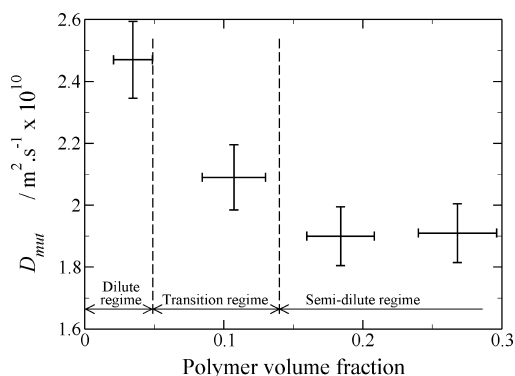
Figure 7. Mutual diffusion coefficient D_{mut} as a function of polymer volume fraction $\bar{\varphi}_p$ in the dilute and semidilute regimes (T = 298 K, polymer from batch 1). Horizontal error bars represent φ_p^{up} and φ_p^{bot}; vertical error bars represent the uncertainty on D_{mut}.

which coefficients have been experimentally fitted. Using our value M_w = 22.4 kg·mol⁻¹, Scholtan's empirical law[11] gives D_0 = $0.84 \cdot 10^{-10}$ m²·s⁻¹ at 298 K, while the laws proposed by François et al.[33] or Patterson et al.[34] at temperature 293 K both lead to $D_0 = 0.61 \cdot 10^{-10}$ m²·s⁻¹. These values are significantly lower than our results presented in Table 5. Nevertheless, the experimental study performed by Patterson et al.[34] shows a rapid increase of the diffusion coefficient in a very short-range of PAAm volume fraction (from 0 to 10^{-3}), so there is no inconsistency with our results.

CONCLUSION

Some thermodynamic properties of polyacrylamide/water solutions have been measured by several techniques. In the concentrated regime, we used gravimetric experiments to obtain the desorption isotherm and the glass transition as a function of temperature from (283 to 328) K. In that range of temperature, the Flory–Huggins interaction parameter in the rubbery regime varies from 0.32 to 0.48, the solvent activity at glass transition from 0.75 to 0.54, and the corresponding solvent volume fraction from 0.30 to 0.18. In the glassy regime, the osmotic bulk modulus K_g increases with temperature, from 1.1 GPa at 283 K to 2.2 GPa at 328 K. The same experimental setup was used to measure the mutual diffusion coefficient at room temperature in the glassy regime. As expected, in this regime, this parameter is strongly dependent on concentration. It increases by two decades and a half when the solvent volume fraction goes up by approximately 0.1 ($D_{mut} = 2.4 \cdot 10^{-14}$ m²·s⁻¹ to $6.6 \cdot 10^{-12}$ m²·s⁻¹ for φ_s = 0.11 to 0.20). The diffusion coefficient has also been measured at high solvent concen-

tration. Since gravimetric techniques fail in that case, due to thermal effects induced by latent heat of vaporization, we used another technique called the sliding symmetric tube, which consists in measuring the concentration as a function of time in two tubes in contact each other. The mutual diffusion coefficient keep the same order of magnitude over the whole range of polymer volume fraction investigated (from 0.035 to 0.25), around $2 \cdot 10^{-10}$ m²·s⁻¹.

AUTHOR INFORMATION

Corresponding Author
*E-mail: frederic.doumenc@upmc.fr.

Notes
The authors declare no competing financial interest.

ACKNOWLEDGMENTS

REFERENCES

(1) Cairncross, R. A.; Jeyadev, S.; Dunham, R. F.; Evans, K.; Francis, L. F.; Scriven, L. E. Modeling and design of an industrial dryer with convective and radiant heating. *J. Appl. Polym. Sci.* **1995**, 58, 1279−1290.
(2) Guerrier, B.; Bouchard, C.; Allain, C.; Bénard, C. Drying kinetics of polymer films. *AIChE J.* **1998**, 44, 791−798.
(3) Allanic, N.; Salagnac, P.; Glouannec, P.; Guerrier, B. Estimation of an effective water diffusion coefficient during infrared-convective drying of a polymer solution. *AIChE J.* **2009**, 55, 2345−2355.
(4) Altinkaya, S. A.; Ozbas, B. Modeling of asymmetric membrane formation by dry-casting method. *J. Membr. Sci.* **2004**, 230, 71−89.
(5) Bassou, N.; Rharbi, Y. Role of Bénard-Marangoni Instabilities during Solvent Evaporation in Polymer Surface Corrugations. *Langmuir* **2009**, 25, 624−632.
(6) Kajiya, T.; Monteux, C.; Narita, T.; Lequeux, F.; Doi, M. Contact-Line Recession Leaving a Macroscopic Polymer Film in the Drying Droplets of Water-Poly(N,N-dimethylacrylamide) (PDMA) Solution. *Langmuir* **2009**, 25, 6934−6939.
(7) Doumenc, F.; Guerrier, B. Drying of a Solution in a Meniscus: A Model Coupling the Liquid and the Gas Phases. *Langmuir* **2010**, 26, 13959−13967.
(8) Huraux, K.; Narita, T.; Frétigny, C.; Lequeux, F. Solution Drying and Phase Separation Morphology of Polyacrylamide/Poly(ethylene glycol)/Water System. *Macromolecules* **2007**, 40, 8336−8341.
(9) Mark, J. E. *Polymer Data Handbook*; Oxford University Press: New York, 1999.
(10) Marcus, Y. *The properties of solvents*; John Wiley and Sons: New York, 1998.
(11) Scholtan, W. Molekulargewichtsbestimmung von Polyacrylamid mittels der Ultrazentrifuge. *Makromol. Chem.* **1954**, 14, 169−178.
(12) Klein, J.; Conrad, K. D. Molecular weight determination of poly(acrylamide) and poly(acrylamide-co-sodium acrylate). *Makromol. Chem.* **1978**, 179, 1635−1638.
(13) Munk, P.; Aminabhavi, T.; Williams, P.; Hohhman, D.; Chmelir, M. Some Solutions Properties of Polyacrylamide. *Macromolecules* **1980**, 13, 871−875.
(14) Riddick, J.; Bunger, W.; Sakano, T. *Organic solvents: physical properties and methods of purification*; John Wiley and Sons: New York, 1986.

(15) Alonso de Mezquia, D.; Blanco, P.; Bou-Ali, M.; Zebib, A. New technique for measuring the molecular diffusion coefficients of binary liquid mixtures. *Proceedings of Eurotherm Seminar 84*, Namur, Belgium, 2009.

(16) Doumenc, F.; Guerrier, B.; Allain, C. Aging and history effects in solvent-induced glass transition of polymer films. *Europhys. Lett.* **2006**, *76*, 630−636.

(17) Doumenc, F.; Bodiguel, H.; Guerrier, B. Physical aging of glassy PMMA/toluene films: Influence of drying/swelling history. *Eur. Phys. J. E* **2008**, *27*, 3−11.

(18) Flory, P. J. *Principles of polymer chemistry*; Cornell University Press: Ithaca, NY, 1995.

(19) Leibler, L.; Sekimoto, K. On the sorption of gases and liquids in glassy polymers. *Macromolecules* **1993**, *26*, 6937−6939.

(20) Saby-Dubreuil, A. C.; Guerrier, B.; Allain, C.; Johannsmann, D. Glass transition induced by solvent desorption for statistical MMA/nBMA copolymers—Influence of copolymer composition. *Polymer* **2001**, *42*, 1383−1391.

(21) Duda, J. L.; Ni, Y. C.; Vrentas, J. S. Toluene diffusion in molten polystyrene. *J. Appl. Polym. Sci.* **1979**, *23*, 947−951.

(22) Doumenc, F.; Guerrier, B.; Allain, C. Mutual diffusion coefficient and vapor-liquid equilibrium data for the system PIB/Toluene. *J. Chem. Eng. Data* **2005**, *50*, 983−988.

(23) Berens, A. Diffusion and relaxation in glassy polymer powders: 1. Fickian diffusion of vinyl chloride in poly(vinyl choride). *Polymer* **1977**, *18*, 697−704.

(24) Sanopoulou, M.; Roussis, P. P.; Petropoulos, J. H. A detailed study of the viscoelastic nature of vapor sorption and transport in a cellulosic polymer. I. Origin and physical implications of deviations from Fickian sorption kinetics. *J. Polym. Sci., Part B: Polym. Phys.* **1995**, *33*, 993−1005.

(25) Dimos, V.; Sanopoulou, M. Anomalous sorption kinetics in the methanol vapor-poly(methyl methacrylate) system. *J. Appl. Polym. Sci.* **2005**, *97*, 1184−1195.

(26) Dubreuil, A.-C.; Doumenc, F.; Guerrier, B.; Johannsmann, D.; Allain, C. Analysis of the solvent diffusion in glassy polymer films using a set inversion method. *Polymer* **2003**, *44*, 377−387.

(27) Dubreuil, A.-C.; Doumenc, F.; Guerrier, B.; Allain, C. Mutual Diffusion in PMMA/PnBMA Copolymer Films: Influence of the Solvent-Induced Glass Transition. *Macromolecules* **2003**, *36*, 5157−5164.

(28) Doumenc, F.; Guerrier, B.; Allain, C. Coupling between mass diffusion and film temperature evolution in gravimetric experiments. *Polymer* **2005**, *46*, 3708−3719.

(29) Doumenc, F.; Guerrier, B. Estimation of the characteristic times of solvent diffusion and polymer relaxation in glassy polymer films by a set inversion method. *Inverse Prob. Sci. Eng.* **2006**, *14*, 747−765.

(30) Long, F.; Richman, D. Concentration gradients for diffusion of vapors in glassy polymers and their relation to time dependant diffusion phenomena. *J. Am. Chem. Soc.* **1960**, *82*, 513−519.

(31) Souche, M.; Long, D. Case-II diffusion and solvent-polymer films drying: A mesoscale model. *Europhys. Lett.* **2007**, *77*, 48002.

(32) Dutrieux, J.; Platten, J.; Chavepeyer, G.; Bou-Ali, M. On the Measurement of Positive Soret Coefficients. *J. Phys. Chem. B* **2002**, *106*, 6104−6114.

(33) Francois, J.; Schwarz, T.; Weill, G. Crossover from the θ to the Excluded Volume Single Chain Statistics: New Experimental Evidences and a Modified Blob Model. *Macromolecules* **1980**, *13*, 564−570.

(34) Patterson, M.; Jamieson, A. Molecular Weight Scaling of the Transport Properties of Polyacrylamide in Water. *Macromolecules* **1985**, *18*, 266−272.